Theoretical study on interband tunneling of holes through GaAs/AlAs/GaAs single-barrier heterostructures

M. Morifuji and C. Hamaguchi

Department of Electronic Engineering, Faculty of Engineering, Osaka University, Yamada-oka, Suita, Osaka 565, Japan
(Received 19 May 1995)

Tunneling of holes through GaAs/AlAs/GaAs single-barrier structures is studied within an elastic multichannel scattering theory. The multiband nature of valence bands requires us to take into account several paths of tunneling between bands with different effective masses, and such an effect of interband tunneling has not been studied as far as we know. Calculated transmission coefficients for GaAs/AlAs/GaAs structures indicate that tunneling current is strongly enhanced due to interband tunneling. We also point out that tunneling current is affected by the phase difference between amplitudes through different paths when in-channel states are coherent. The possibility of such a interference effect is discussed.

I. INTRODUCTION

Since the development of artificial superlattices, tunneling phenomena in semiconductor nanostructures have attracted much interest and a large number of studies have been made for tunneling in various structures. In addition to tunneling itself, various effects such as phonons, impurities interface roughness, etc., on tunneling current have been also studied.[1-3] However, most of the studies have been devoted to tunneling of electrons in the conduction band with n-doped electrodes. On the other hand, tunneling of holes has been rarely studied theoretically or experimentally. One reason for this situation is due to the fact that holes have heavier effective masses than electrons in most semiconductors. From a viewpoint of device development, the heavy effective mass of holes is unfavorable, in contrast to electrons whose light effective mass attracts much interest for device applications.[4-6]

In addition to the difference in effective masses, there is an essential difference between electrons and holes of a zinc-blende-type semiconductor; electrons populate only one band while holes distribute in two bands: the heavy-hole band and the light-hole band. Such a multiband nature of valence bands may make the tunneling phenomena quite complicated. There should be a mixing between the states with different effective masses when the translational symmetry is broken due to a heterojunction or a potential drop, since the effective mass specifies a state only when a translational symmetry exists. The effect of interband mixing will be larger for holes than for electrons because of the multiband nature. Thus, for hole tunneling, there should exist tunneling paths between bands with different effective masses in addition to the ones between the same bands. We have to take the mixing between different band into account accurately when we consider the hole tunneling. Such a band mixing effect on tunneling current flowing across nanostructures has not been studied. Although the situation is very complicated, the interband tunneling may result in recognizable phenomena.

In this paper, we pay attention to the interband mixing of hole states and we theoretically study the effect of interband tunneling of holes through single-potential barriers, neglecting some important effects such as phonons, interface roughness, and so on. Although these effects are also important for hole tunneling, we expect that the features of hole tunneling presented in this paper will appear even in the presence of the other effects.

II. THEORY OF HOLE TUNNELING

A. Theory of hole tunneling

We calculate current density flowing through a potential barrier within an elastic scattering theory.[7,8] The system we consider is a [100] GaAs/AlAs/GaAs single-barrier structure with p-type doped three-dimensional electrodes.

Figure 1 shows a schematic band structure of the valence band of the system under an applied voltage. Holes are injected from one electrode of GaAs (denoted by I) and tunnel through the AlAs barrier region (denoted by II) to another GaAs electrode (denoted by III) with a certain probability. In this paper, we consider the case where electric field, which is assumed to be homogeneous, is applied only to region II. Since states far away from the barrier can be treated as in equilibrium, states in the electrodes are well described as bulk states. Thus the in-channel states in region I and out-channel states in region III are treated as bulk states. In both regions I and III, two bands with different effective masses lie at the valence band edge, i.e., a heavy-hole (hh) band and a light-hole (lh) band, which are shown in Fig. 1 by parabolic curves. In addition to them, the spin-orbit split-off (so) band lies 0.34 eV below from the valence band edge. In an equilibrium, holes are distributed in both of hh band and lh band (schematically denoted by the thick part of the curves) with a ratio of density of states for each band.

There are several methods for calculation of the tun-
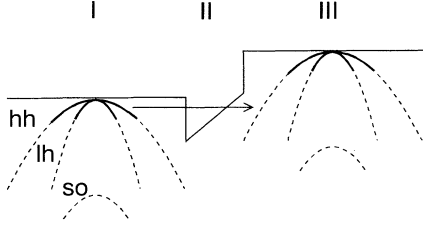
<u>52</u>   14 131

FIG. 1. Schematic picture of the band structure of the system. Parabolic curves denote the hh, lh, and so bands, whose thick part indicates the region where holes exist. Holes in region I tunnel to region III through the potential barrier.

neling current, the WKB method, transfer Hamiltonian,[9] transfer matrix,[10,11] the Wigner function method,[12] and so on. These methods are usually based on the framework of an effective mass approximation and have succeeded in explaining the behavior of electron tunneling phenomena. For holes, however, the effective mass approximation will be inadequate to describe the tunneling between different effective masses. On the other hand, a tight-binding theory easily describes the interband mixing because no effective mass is used for specifying states.[13,14] For example, direct-pseudodirect transition (crossover between a Γ-like state and an X-like state) in the $(GaAs)_n/(AlAs)_n$ superlattices is well explained by a second-neighbor tight-binding calculation.[15] Furthermore, Γ-X mixing in short-period GaAs/AlAs superlattices in the presence of an electric field is well described by the tight-binding theory, and the observed behavior of Stark ladders in short-period superlattices is well explained.[16-18]

In this paper, we evaluate current density based on an elastic multichannel scattering theory employing transmission amplitudes, which are calculated using the theory developed by Schulman and co-workers.[19-21] This method is based on the tight-binding picture, and has an ability to introduce the interband mixing associated with a heterojunction or a potential drop. Furthermore, this method has the ability to describe realistic band structures and a flexibility for any potential energies at atomic layers.[22,23] We have adopted tight-binding parameters empirically obtained by Vogl et al. for $sp^3 s^*$ orbitals,[24] and an intra-atomic spin-orbit interaction obtained by Chadi.[25] For a good description of conduction bands, some authors have presented sets of tight-binding parameters by extending the interaction up to the second-neighboring atoms,[26-28] however, we can expect a good description for the valence band within a simple picture of first-neighbor interactions.

We briefly review the method here.[19,20] In regions I and III, a bulk state is specified by its energy E and a two-dimensional wave vector along the interface $k_{\parallel}$. Here the terminology "bulk state" includes imaginary (evanescent) states with complex wave vectors in addition to real (Bloch) states. A vector t_{I} (t_{III}) consists of the amplitudes of the bulk states in region I (III). The t_{I} (t_{III}) depends on E and $k_{\parallel}$, although the dependence is not explicitly

shown. The t_{I} (t_{III}) is organized so that the top half includes the coefficient of rightward propagating real state and rightward decaying complex states. The bottom half of the t_{I} (t_{III}) is for the leftward propagating real states and leftward decaying complex states. This is written as $t_{\mathrm{I}} = (t_{\mathrm{I}}^+(i),\ t_{\mathrm{I}}^-(i))$ and $t_{\mathrm{III}} = (t_{\mathrm{III}}^+(i), t_{\mathrm{III}}^-(i))$ with the index $i = 1$-5 for the $sp^3 s^*$ basis. These coefficients are related with each other by a transfer matrix M as

$$\begin{bmatrix} t_{\mathrm{III}}^+ \\ t_{\mathrm{III}}^- \end{bmatrix} = \begin{bmatrix} M_{++} & M_{+-} \\ M_{-+} & M_{--} \end{bmatrix} \begin{bmatrix} t_{\mathrm{I}}^+ \\ t_{\mathrm{I}}^- \end{bmatrix}, \tag{1}$$

with

$$\begin{bmatrix} M_{++} & M_{+-} \\ M_{-+} & M_{--} \end{bmatrix} \equiv S_{\mathrm{III}}^{\dagger}(k_{\parallel}, E - V) \prod_j T_j(k_{\parallel}, E - V_j)$$

$$\times S_{\mathrm{I}}(k_{\parallel}, E). \tag{2}$$

In Eq. (2), $T_j(k_{\parallel}, E - V_j)$ is a matrix that connects amplitudes of atomic orbitals in the jth layer with those of adjacent layers and j runs through all atomic layers in region II. V is a total potential drop through region II and V_j is a potential energy at the jth layer. $S_{\mathrm{I}}(k_{\parallel}, E)$ $[S_{\mathrm{III}}(k_{\parallel}, E)]$ denotes bulk states eigenvectors in region I (III). By solving Eq. (1), we can obtain the tunneling amplitude from the nth band in region I to the n'th band in the region III, $t_{n,n'}$ (n and n' denote the hh, lh, and so states). In calculation, we set t_{I}^+ as

$$t_{\mathrm{I}}^+(i) = \begin{cases} 1 & (\text{for}\ \ i = n) \\ 0 & (\text{others}), \end{cases} \tag{3}$$

so as to specify the in-channel state. Solving Eq. (1) with a boundary condition $t_{\mathrm{III}}^- = 0$ and Eq. (3), we obtain the tunneling amplitudes t_{III}^+ of which the n'th component is regarded as $t_{n,n'}$.

Using the calculated tunneling amplitudes, the current density is calculated as

$$j(V) = \frac{2e}{(2\pi)^3 \hbar} \sum_{n,n'} \int d^2 k_{\parallel} \int dE \left[|t_{n,n'}|^2 \frac{v_{n'k'}}{v_{nk}} \right]$$

$$\times [f_{\mathrm{III}}(E_{n'k'} - V) - f_{\mathrm{I}}(E_{nk})]. \tag{4}$$

In Eq. (4), v_{nk} ($v_{n'k'}$) is a velocity of an in-channel (out-channel) state, and $f_{\mathrm{I}}(E_{nk})$ and $f_{\mathrm{III}}(E_{n'k'})$ are the Fermi distribution function in regions I and III, respectively. In this paper, we consider the case where the hole density is high enough to degenerate. Furthermore, we assume that the temperature is low enough so as to regard the Fermi distribution function as a step function.

B. Interference effect

For tunneling from single band to single band, the phase of tunneling coefficient is trivial because only an absolute value of tunneling coefficient contributes to current density. However, when we consider multichannel tunneling, the phase change during tunneling may have an important roll because amplitudes from the two in-channel states interfere. Thus, we may expect that the phase difference between tunneling states can be observed if the two in-channel states are coherent.
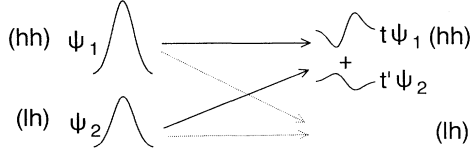
THEORETICAL STUDY ON INTERBAND TUNNELING OF ...

FIG. 2. Schematic picture of interference effect of hole tunneling. In-channel states from hh (ψ_1) receive a certain phase factor during tunneling. In-channel states from lh (ψ_2) also receive a phase factor different from that of ψ_1. Since the out-channel state is a superposition of $t\psi_1$ and $t'\psi_2$, the out-flowing current is affected by the phase difference between $t\psi_1$ and $t'\psi_2$.

We consider two tunneling paths from two different states to one state such as hh-hh and lh-hh as shown by arrows in Fig. 2. Since transmission coefficients t's are complex numbers, t's can be written as $t_{n,n'} = |t_{n,n'}|e^{i\phi_{n,n'}}$. The phase factor $\phi_{n,n'}$ is regarded as a phase shift of a wave function during tunneling. If two in-channel states from hh and that from lh are coherent, that is, they have a certain phase difference, an out-channel hh state will be a superposition of two kinds of components as $|t\psi_1 + t'\psi_2|^2$ instead of $|t\psi_1|^2 + |t'\psi_2|^2$. These two expressions result in different states when $|t|^2$ and $|t'|^2$ are of the same order. Thus the interference effect will be seen; tunneling current density is affected by the phase difference between $t\psi_1$ and $t'\psi_2$. In this case, the phase difference of in-channel states will be important. If we assume the same phase for in-channel states, the tunneling current would be expressed as

$$j(V) = \frac{2e}{(2\pi)^3\hbar} \sum_{n'} \int d^2k_\parallel \int dE \left[\left| \sum_n t_{n,n'} \right|^2 \frac{v_{n'k'}}{v_{nk}} \right]$$
$$\times [f_{II}(E_{n'k'} - V) - f_I(E_{nk})], \quad (5)$$

instead of Eq. (4). Although it is a crucial problem whether the coherency of in-channel states is realized in real systems, we may expect it when the electrodes are very small with very flat interfaces.

III. RESULTS AND DISCUSSION

In this section, we show calculated results for a GaAs/AlAs/GaAs single-barrier structure. We used the valence band offset between GaAs and AlAs 0.55 eV.[26] Figure 3 shows calculated transmission coefficients $|t_{n,n'}|^2$ for a state $k_\parallel = 0$ of GaAs/(AlAs)$_{10}$/GaAs structure as functions of the in-channel state energy for applied voltage 0 V. The curves have qualitative features similar to a curve calculated by Mendez[29] for electron tunneling within the effective mass approximation. For lower energies where holes distribute, $|t_{lh,lh}|^2$ is larger than others, reflecting the light effective mass. Comparing with $|t_{lh,lh}|^2$, other components are rather small and in almost the same order. Light-hole related tunneling probabilities, $|t_{lh,lh}|^2$, $|t_{lh,hh}|^2$ and $|t_{hh,lh}|^2$ show a singularity at 0.34 eV where the band edge of the so band lies
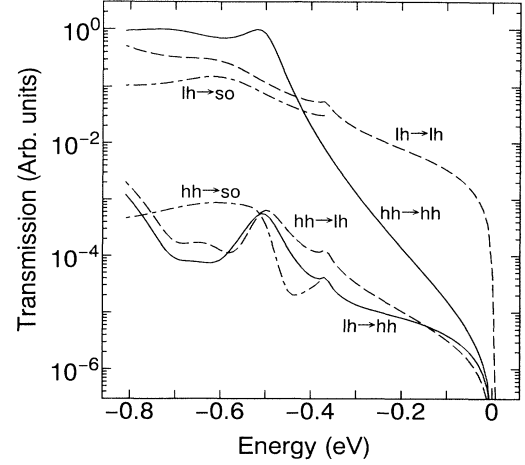

FIG. 3. The calculated transmission coefficients $|t_{n,n'}|^2$ for the GaAs/(AlAs)$_{10}$/GaAs single-barier structure as functions of in-channel state energy for applied voltage 0 V.

at, while $|t_{hh,hh}|$ has no singularity. This is because the lh band and the so band are of similar nature: s and p_z atomic orbitals. These components depend exponentially on the in-channel state energy. This indicates that the tunneling from the Fermi energy states in region I contributes most to the tunneling current.

The applied voltage dependence of the transmission coefficients for in-channel state energy -0.02 eV is shown in Fig. 4. This energy corresponds to the Fermi energy when hole density is about 1.0×10^{19} cm^{-3}. We can see that $|t_{lh,lh}|^2$ is the largest of all at any applied voltage. $|t_{hh,hh}|^2$ is small at small voltage, while it becomes important when the voltage is larger than 1 V. $|t_{lh,so}|^2$ has also a large value, but tunneling related to the so band contributes little to current density. This is because the so states have smaller k vector than the hh and lh states

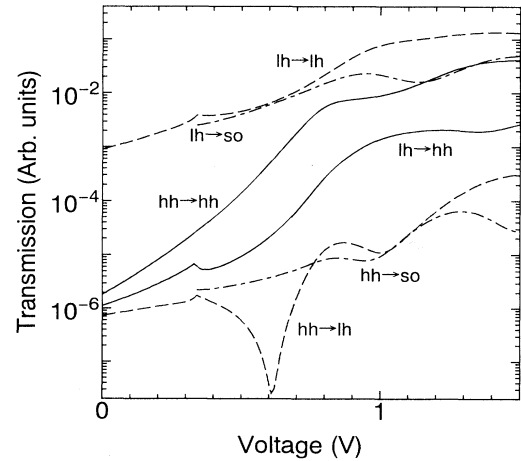FIG. 4. The calculated transmission coefficients $|t_{n,n'}|^2$ for GaAs/(AlAs)$_{10}$/GaAs as functions of applied voltage.

at the same energy. Other interband components are small at any voltage.

Behavior of interband tunneling probability can be estimated easily. When the tunneling coefficient is very small, we can estimate interband tunneling probability using the effective mass approximation as

$$|t_{n,n}|^2 \sim e^{-\alpha\sqrt{m_n^*}}, \qquad (6)$$

with $\alpha = 2\sqrt{2(V_0 - E)}d/\hbar$, where V_0 and d are barrier height and barrier width, respectively. Substituting the effective masses of GaAs ($m_{hh} = 0.51m_0$ and $m_{lh} = 0.082m_0$, where m_0 is the electron mass) and $V_0 = 0.55$ eV into Eq. (6), we obtain $|t_{hh,hh}|^2/|t_{lh,lh}|^2 \sim 10^{-4}$ for GaAs/(AlAs)$_{10}$/GaAs. While, from Fig. 4 we see that $|t_{hh,hh}|^2/|t_{lh,lh}|^2 \sim 10^{-3}$, which is larger than the value estimated by the effective mass approximation. This discrepancy arises from the band nonparabolicity, which is neglected in the simple effective mass approximation. As the voltage increases, $|t_{hh,hh}|^2$ becomes larger comparing with $|t_{lh,lh}|^2$. This is explained from Eq. (6) qualitatively in terms of the decrease in α associated with barrier narrowing with increasing voltage.

Electric field in the barrier region increases with increasing voltage and the interband mixing during tunneling will be induced by the electric field. Thus, as for interband components, we may expect that interband tunneling becomes important with increasing voltage. However, the calculated results show that the electric field induced mixing between the hh and lh states is not so large and that interband components remain smaller than intraband components even at larger voltage.

All of the tunneling coefficients show oscillatory behavior with increasing voltage. The oscillation occurs associated with barrier narrowing due to applied voltage and is known as Fowler-Nordheim tunneling.

Dependence of $|t_{n,n'}|^2$ on $k_{\parallel}$ is shown in Fig. 5. The intraband tunneling coefficients $|t_{hh,hh}|^2$ and $|t_{lh,lh}|^2$ show a very weak variation with $k_{\parallel}$. This feature of the intraband tunneling may allow us to evaluate tunneling
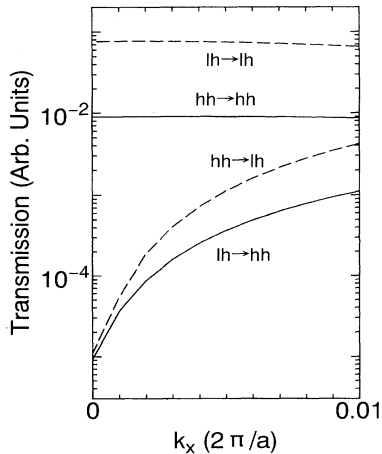
current only at $k_{\parallel} = 0$ as usually done for the case of electron tunneling. On the other hand, interband tunneling coefficients increase rapidly as $k_{\parallel}$ increases. This is because mixing between the hh and lh in-channel states becomes larger with $k_{\parallel}$ apart from the Γ point. This behavior of interband tunneling coefficients requires us to take $k_{\parallel}$ integration carefully in evaluating tunneling current and indicates that the interband tunneling should not be neglected for hole tunneling.

In Fig. 6, the phase difference, $\phi_{hh,hh} - \phi_{lh,hh}$, $\phi_{hh,lh} - \phi_{lh,lh}$, and $\phi_{hh,so} - \phi_{lh,so}$ are plotted by a solid, broken, dot-dashed curve, respectively. From the calculation, we have found that the phase changes are different for each different tunneling paths. Moreover, the phase difference is a function of the applied voltage. The phase difference shows oscillation, which coincides with the Fowler-Nordheim oscillation of tunneling probability. Figure 7 shows $k_{\parallel}$ dependence of the phase change for some tunneling paths. $\phi_{n,n'}$ for intraband tunneling show even function dependence with very weak variation, while $\phi_{n,n'}$ for interband tunneling show odd functionlike variation.

Current density vs applied voltage calculated for GaAs/(AlAs)$_{10}$/GaAs is shown in Fig. 8, where we assumed the hole density in the regions I and III to be 1.0×10^{19} cm^{-3}. In this figure the broken curve shows the current density evaluated by using Eq. (4) where the interband tunneling is considered. The dot-dashed curve shows the current density where the interband tunneling is neglected. From these curves, we see that interband mixing considerably enhances tunneling current. The solid curve is the current density when the coherency of in-channel states, is assumed. The interference effect noted in Sec. 2 results in an enhancement of current density. We have to note that the interference effect depends on the phase difference between in-channel states, which is assumed to be zero in the calculation.
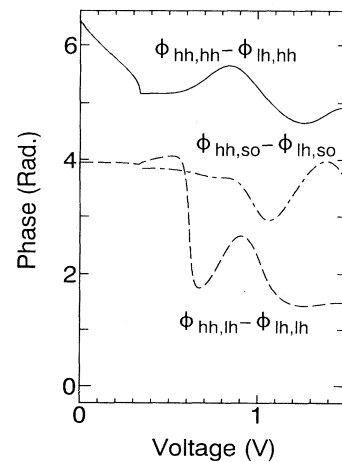

FIG. 5. The calculated transmission coefficients $|t_{n,n'}|^2$ for GaAs/(AlAs)$_{10}$/GaAs as functions of $k_{\parallel}$.

FIG. 6. The phase difference between amplitudes of out-channel states $\phi_{n,n'} - \phi_{n',n'}$ calculated for the GaAs/(AlAs)$_{r10}$/ GaAs single-barrier structure as functions of applied voltage.
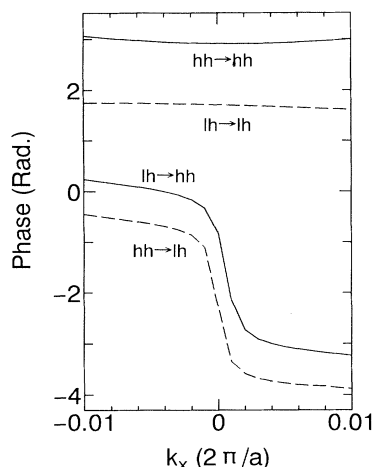
FIG. 7. The phase difference of out-channel states $\phi_{n,n'}$ calculated for the GaAs/(AlAs)$_{10}$/GaAs single-barrier structure as functions of $k_\parallel$.

FIG. 8. The calculated tunneling current density for GaAs/(AlAs)$_{10}$/GaAs as functions of the applied voltage. The broken (dot-dashed) curve shows the current density where the interband tunneling is considered (neglected). The solid curve is the current density when the coherency of the in-channel states is assumed.

In summary, we theoretically studied tunneling of holes through a GaAs/AlAs/GaAs single-barrier structure within tight-binding theory taking interband mixing and interband tunneling into account. The calculated results show that the interband tunneling coefficients have large value and thus tunneling current is enhanced due to interband tunneling. We also pointed out that phase difference between tunneling paths affects the tunneling current. This indicates a possibility of interference effect, that is, the phase of wave function affects observed tunneling current. From the calculation, we found that the phase change during tunneling depends on applied voltage. The calculated results show that $k_\parallel$ dependence of tunneling coefficients is important for accurate evaluation of tunneling current. On the other hand, contribution from many $k_\parallel \neq 0$ states may be unfavorable for in-channel states coherency.

In this paper, we considered an ideal case neglecting such effects as phonons, interface roughness, and so on, which are important in the real system. We adopted a simple picture for tunneling probability where the distribution function is not changed during tunneling. Some authors carried out calculations of tunneling current using the Wigner functions and report that the
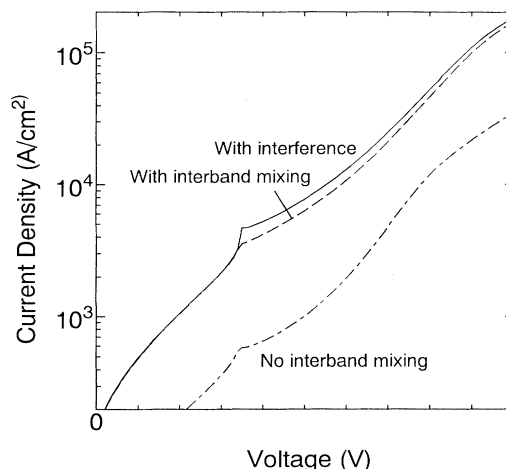
current-voltage characteristics are affected by a change of the Fermi distribution function due to a potential barrier.[12,30] These effects may change the results presented in this paper quantitatively. Thus, comparison with experiment will be necessary to clarify whether the interband tunneling will contribute to the tunneling current or not. We expect, however, that the features of hole tunneling presented in this paper will contribute to the tunneling current even in the presence of the such effects.

ACKNOWLEDGMENTS

[1] A. D. Braisford and L. C. Davis, Phys. Rev. B **2**, 1708 (1970).
[2] N. Mori and C. Hamaguchi, Semicond. Sci. Technol. **8**, 176 (1993).
[3] K. Hirakawa, Phys. Rev. B **40**, 3451 (1989).
[4] M. Tsuchiya and H. Sakaki, Appl. Phys. Lett. **49**, 88 (1986).
[5] M. Tsuchiya and H. Sakaki, Appl. Phys. Lett. **50**, 1503 (1986).
[6] A. R. Bonnefoi, D. H. Chow, and T. C. McGill, J. Appl. Phys. **62**, 3836 (1987).
[7] A. Di Carlo, P. Vogl, and W. Pötz, Phys. Rev. B **50**, 8358 (1994).
[8] A. Di Carlo and P. Vogl, Semicond. Sci. Technol. **9**, 497 (1994).
[9] M. C. Payne, J. Phys. C. **19**, 1145 (1986).
[10] E. O. Kane, Tunneling Phenomena in Solids (Plenum, New York, 1969), Chap. 1.
[11] Y. Ando and T. Itoh, J. Appl. Phys. **61**, 1497 (1987).
[12] W. R. Frensley, Phys. Rev. B **36**, 1570 (1987).
[13] H. Akera, S. Wakahara, and T. Ando, Surf. Sci. **196**, 694

(1988).

[14] T. B. Boykin, J. P. A. van der Wagt, and J. S. Harris, Phys. Rev. B **43**, 4777 (1991).

[15] T. Matsuoka, T. Nakazawa, T. Ohya, K. Taniguchi, C. Hamaguchi, H. Kato, and Y. Watanabe, Phys. Rev. B **43**, 11 798 (1991).

[16] M. Morifuji, M. Yamaguchi, K. Taniguchi, and C. Hamaguchi, Phys. Rev. B **50**, 8722 (1994).

[17] M. Yamaguchi, H. Nagasawa, M. Morifuji, K. Taniguchi, C. Hamaguchi, C. Gmachl, and E. Gornik, Semicond. Sci. Technol. **9**, 1810 (1994).

[18] A. J. Shields, P. C. Klipstein, M. S. Skolnick, G. W. Smith, and C. R. Whitehouse, Phys. Rev. B **42**, 5879 (1990).

[19] J. N. Schulman and Y.-C. Chang, Phys. Rev. B **27**, 2346 (1983).

[20] J. N. Schulman and D. Z.-Y. Ting, Phys. Rev. B **45**, 6282 (1992).

[21] Y.-C. Chang and J. N. Schulman, Phys. Rev. B **25**, 3975

(1982).

[22] J. A. Støvneng, E. H. Hauge, P. Lipavský, and V. Špička, Phys. Rev. B **44**, 13 595 (1991).

[23] M. Morifuji, Y. Nishikawa, C. Hamaguchi, and T. Fujii, Semicond. Sci. Technol. **7**, 1047 (1992).

[24] P. Vogl, H. P. Hjalmarson, and J. D. Dow, J. Phys. Chem. Solids **44**, 365 (1983).

[25] D. J. Chadi, Phys. Rev. B **16**, 790 (1977).

[26] Yan-Ten Lu and L. J. Sham, Phys. Rev. B **40**, 5567 (1989).

[27] Jian-Bai Xia and Yia-Chung Chang, Phys. Rev. B **42**, 1781 (1990).

[28] K. E. Newmann and J. D. Dow, Phys. Rev. B **36**, 1929 (1984).

[29] E. E. Mendez, in *Physics and Applications of Quantum Wells and Superlattices*, edited by E.E. Mendez and K. von Klitzing (Plenum, New York, 1988), p. 159.

[30] D. D. Coon and H. C. Liu, Appl. Phys. Lett. **47**, 172 (1985).